

Infrared Hall effect in the electron-doped high- T_c cuprate $\text{Pr}_{2-x}\text{Ce}_x\text{CuO}_4$

A. Zimmers,¹ L. Shi,^{2,*} D. C. Schmadel,² W. M. Fisher,¹ R. L. Greene,¹ H. D. Drew,^{2,†} M. Houseknecht,³ G. Acbas,³ M.-H. Kim,³ M.-H. Yang,³ J. Cerne,³ J. Lin,⁴ and A. Millis⁴

¹Center for Superconductivity Research, Department of Physics, University of Maryland, College Park, Maryland 20742, USA

²Department of Physics, University of Maryland, College Park, Maryland 20742, USA

³Department of Physics, University at Buffalo, SUNY, Buffalo, New York 14260, USA

⁴Physics Department, Columbia University, New York, New York 10027, USA

(Received 2 February 2007; revised manuscript received 30 May 2007; published 14 August 2007)

The electron-doped cuprate $\text{Pr}_{2-x}\text{Ce}_x\text{CuO}_4$ is investigated using infrared magneto-optical measurements. The optical Hall conductivity $\sigma_{xy}(\omega)$ shows a strong doping, frequency, and temperature dependence consistent with the presence of a temperature- and doping-dependent coherent backscattering amplitude which doubles the electronic unit cell and produces a spin density wave state. At low temperatures, the data suggest that the coherent backscattering vanishes at a quantum critical point inside the superconducting dome and is associated with the commensurate antiferromagnetic order observed by other workers. Using a spectral weight analysis, we have further investigated the Fermi-liquid-like behavior of the overdoped sample. The observed Hall-conductance spectral weight is about ten times less than that predicted by band theory, raising the fundamental question of the effect of Mott and antiferromagnetic correlations on the Hall conductance of strongly correlated materials.

DOI: 10.1103/PhysRevB.76.064515

PACS number(s): 74.25.Gz, 74.72.Jt, 75.30.Fv, 75.40.-s

The physics of doped Mott insulators is believed to underlie the exotic properties of many “strongly correlated” materials.¹ Among these, the properties of cuprates remain one of the greatest challenges in condensed matter physics. The last few years have seen remarkable progress in the synthesis of high-critical-temperature (high- T_c) cuprates, followed by reliable and high-performance energy and momentum spectroscopic measurements. It is now possible to compare quantitatively the electron-doped side and the hole-doped side in the cuprate phase diagram. One striking difference is the presence of antiferromagnetic order in a much larger region on the electron-doped side of the phase diagram. This characteristic has been seen directly by neutron scattering,^{2,3} muon spin resonance,⁴ and indirectly by optics^{5,6} and angle-resolved photoemission spectroscopy (ARPES).⁷⁻⁹ However, the exact location of the antiferromagnetic (AF) region with respect to the superconducting region remains an open question, as does the effect of antiferromagnetic order and fluctuations on electronic properties. ARPES (Refs. 7–9) and optical⁵ studies have shown the presence of a large energy pseudogap in superconducting samples which disappears at high temperatures. The nature of this gap is a central issue in cuprate physics and is currently under intense debate. In one scenario, it is considered to be the signature of the coexistence of AF order and superconductivity.¹⁰ The optical signature of this gap in the optimally doped sample is, however, not seen directly in the spectral response, but is revealed indirectly when analyzing the partial sum rule of σ_{xx} at this doping. In addition, recent inelastic neutron studies³ have concluded that long-range AF and superconductivity orders do not overlap, by showing that the antiferromagnetic correlation length never diverges in superconducting samples.

To test if antiferromagnetic signatures can clearly be seen in the electronic response of superconducting samples, and most importantly up to optimal doping, we have performed infrared Hall (ir Hall) measurements of the electron-doped

cuprate $\text{Pr}_{2-x}\text{Ce}_x\text{CuO}_4$ (PCCO) over a wide range of dopings and temperatures. Indeed ir Hall measurements have been found to be an extremely sensitive probe of the strong correlation effects in the hole-doped cuprates,¹³⁻¹⁵ which can reveal more about the electronic structure of materials than the longitudinal conductivity σ_{xx} . As expected, we find a rich structure in σ_{xy} of PCCO. At low temperatures, we find clear evidence of a gaplike feature in underdoped samples still present at optimal doping, and disappearing in the overdoped sample. These findings support the scenario of a reconstruction of the Fermi surface in the electron-doped cuprates due to antiferromagnetic ordering, and the presence of a quantum critical point inside the superconducting dome. We find that this general picture is, however, not complete since it cannot explain the underdoped response at high temperature and the spectral weight analysis of overdoped samples.

Thin films of $\text{Pr}_{2-x}\text{Ce}_x\text{CuO}_4$ of several compositions were grown on LaSrGaO_4 (LSGO) substrates using pulsed laser deposition.¹⁶ In this experiment we have studied the following samples: a highly underdoped sample ($x=0.12$) $T_c=2$ K (thickness 1260 Å), an optimally doped sample ($x=0.15$) $T_c=19.6$ K (thickness 1450 Å), and an overdoped sample ($x=0.18$) $T_c=9.3$ K (thickness 1250 Å). We have measured the reflectance (R), transmittance (T), and complex Faraday angle. From these we have extracted the longitudinal conductivity (σ_{xx}) and Hall conductivity (σ_{xy}). The reflectance and transmittance were measured for all samples in the 1200–4000 cm^{-1} spectral range with a Bomem Fourier transform spectrometer, at five temperatures between 30 and 300 K using a continuous flow cryostat. The frequency and temperature dependence of the LSGO substrate index of refraction was measured separately. Using this index and the experimental R and T data of the entire sample (PCCO/LSGO), one can extract the solution for the complex conductivity σ_{xx} of PCCO. Errors generated using this method are estimated to be less than 5% and are primarily due to the

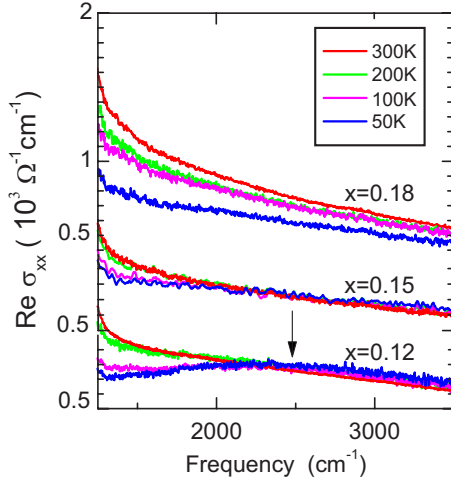


FIG. 1. (Color online) Optical conductivity of PCCO, $x=0.12$, 0.15 , and 0.18 (curves are shifted from one another by 0.5 for clarity). The underdoped sample and optimally doped samples show evidence of a high-energy gap. This feature is accompanied by a transfer of spectral weight from low to high energy when the temperature is lowered below a characteristic temperature T_W . This partial gap feature is no longer seen in the overdoped sample, which can be modeled using an extended Drude model.

values used for the thickness of the substrate and the film (the latter was measured by Rutherford backscattering). Figure 1 shows the frequency and temperature dependence of σ_{xx} determined using this method.^{17,18} One can clearly distinguish two very different behaviors as temperature is lowered from 300 to 20 K. For $x=0.12$, below a characteristic temperature $T_W \approx 200$ K, one can observe a dip and peak formation around 2500 cm^{-1} (see the arrow in Fig. 1). As shown previously, this feature is also followed by a transfer of spectral weight from low to high energy as the temperature is lowered.^{5,6} This transfer is thought to be the signature of a partial gap opening on the Fermi surface, as seen by ARPES measurements. A spin density wave model⁵ was suggested to explain this data. This dip and peak formation can no longer clearly be seen for $x=0.15$. However, a careful analysis of the optical conductivity sum rule reveals the presence of a partial gap at this doping as well.⁵ Unlike the results for $x=0.12$ and 0.15 , the optical conductivity of PCCO $x=0.18$ does not show any signature of a partial gap opening and can be described using an extended Drude model as the temperature is lowered. Results presented in Fig. 1 are thus consistent with previous published results:⁵ a partially gapped Fermi surface is observed optically on the underdoped side, and a marginal Fermi liquid behavior on the overdoped side of the phase diagram.

The Faraday rotation and ellipticity, represented by the complex Faraday angle θ_F were measured at several ir laser frequencies using a photoelastic polarization modulation technique^{20,21} from 30 to 300 K and from -8 to 8 T. Experimental errors generated by this analysis in the real and imaginary parts of σ_{xy} due to errors in measurements of σ_{xx} and θ_F are estimated to be $\pm 5\%$. Using the measured values of σ_{xx} , the Faraday angle θ_F can be translated into other response functions, such as the infrared Hall conductivity σ_{xy}

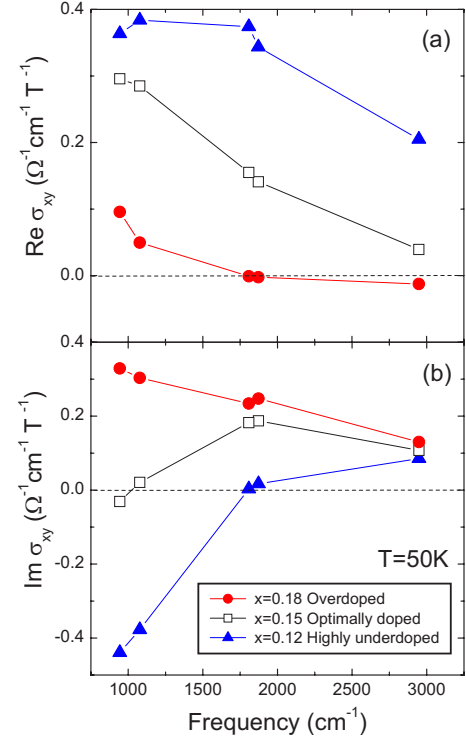


FIG. 2. (Color online) (a) Real and (b) imaginary parts of σ_{xy} as functions of frequency at 50 K. Qualitatively, the overdoped $x=0.18$ sample shows a holelike extended Drude response plotted in Fig. 3. The underdoped $x=0.12$ and optimally doped $x=0.15$ samples show, however, a clear inconsistency with this model, such as a sign change in $\text{Im}(\sigma_{xy})$. As described in the text and as shown in Fig. 3, these features are due to the presence of antiferromagnetic order in the sample.

(the off-diagonal term in the complex conductivity tensor $\tilde{\sigma}$) using²¹

$$\tan \theta_F \approx \frac{\sigma_{xy}}{\sigma_{xx}} \left(1 + \frac{1}{Z\sigma_{xx}} \right)^{-1}, \quad (1)$$

where $Z = (Z_0 d) / (n_s + 1)$, Z_0 is the impedance of free space, n_s is the refractive index of the substrate, and d is the thickness of the PCCO film. Previous studies have validated this technique by measuring the ir Hall response of simple metals such as gold and copper.²² The ir Hall spectra for these cases were found to be consistent with a Drude model using the mass parameter taken from band theory and the measured scattering rate from σ_{xx} .

Figure 2 shows our principal results: the real and imaginary parts of σ_{xy} as a function of frequency for $x=0.12$, 0.15 , and 0.18 at $T=50$ K. We begin our discussion of these data with reference to the extended Drude model:

$$\sigma_{xy} = \frac{S_{Mott}}{\{\gamma(\omega) - i\omega[1 + \lambda(\omega)]\}^2} \quad (2)$$

with $\gamma(\omega)$ and $1 + \lambda(\omega)$ the frequency-dependent scattering rate and effective mass, respectfully. This model is plotted in Fig. 3 (red circle symbols), using $\gamma(\omega)$ and $\lambda(\omega)$ determined by previous σ_{xx} measurements⁵ and S_{Mott} , the total Drude

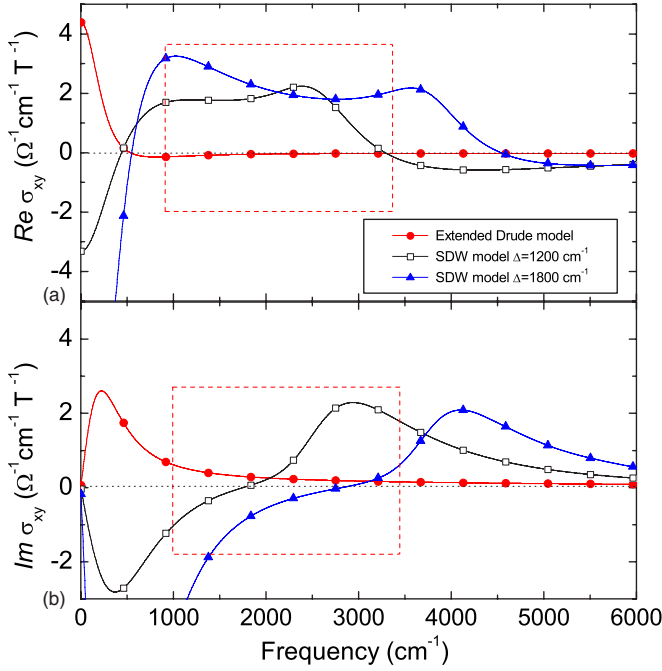


FIG. 3. (Color online) (a) Real and (b) imaginary parts of σ_{xy} as a function of frequency for a hole-doped extended Drude model and a spin density wave (SDW) model with two different gap values. As observed experimentally in Figs. 2 and 4, the calculated zero-crossing frequency decreases with smaller input gap values Δ in the SDW model (see dashed boxes for better comparison).

spectral weight, determined by the band structure renormalized due to Mott physics (this value will be discussed at length in the last part of the paper). In this model, $\text{Im}(\sigma_{xy})$ has the same sign at all frequencies, while $\text{Re}(\sigma_{xy})$ has one sign change at a frequency set by $\gamma(\omega)$. The $x=0.18$ data in Fig. 2 are qualitatively consistent with this extended Drude model: $\text{Im}(\sigma_{xy})$ has the holelike signature predicted by the band structure and does not change sign over the experimentally accessible frequency range; at low frequencies, $\text{Re}(\sigma_{xy})$ has the holelike sign found in the dc Hall measurement,¹¹ along with one sign change (at $\approx 1750 \text{ cm}^{-1}$) in the experimental frequency range. One qualitative inconsistency with the extended Drude model is that the calculated zero crossing occurs well below the experimental zero crossing. We believe that this difference could be due to antiferromagnetic correlations which produce electronlike contributions to σ_{xy} below the frequency range of our measurements. From Kramers-Kronig relations, these low-frequency contributions would increase $\text{Re}(\sigma_{xy})$ (thus pushing the zero crossing to higher frequencies) while doing little to $\text{Im}(\sigma_{xy})$ in our frequency range. Evidence for antiferromagnetic correlations is also seen as multiple zero crossings of R_H with temperature in the dc Hall coefficient in similarly doped samples.¹¹ To summarize the $x=0.18$ response, the rough magnitude and frequency dependence predicted by the model are in qualitative accord with the measurement, but the incorrect position of the zero crossing in $\text{Re}(\sigma_{xy})$ demonstrates that, despite its success in fitting the longitudinal conductivity,⁵ the extended Drude model is an inadequate description of transport even

in overdoped PCCO. This inconsistency will be further addressed in the last part of this paper.

The IR Hall data we have for $x=0.12$ and 0.15 differ qualitatively from the predictions of the Drude model: (i) $\text{Im}(\sigma_{xy})$ exhibits zero crossings at frequencies which increase as doping decreases; (ii) $\text{Re}(\sigma_{xy})$ is concomitantly larger and positive. Since dc Hall measurements¹¹ indicate an electronlike sign for both of these dopings, this implies that a sign change must also occur below our lowest measured frequency in $\text{Re}(\sigma_{xy})$. It is striking that, contrary to σ_{xx} data (where only partial sum rule arguments enable us to reveal a high-energy gap), our raw σ_{xy} data directly show a clear departure from the Drude model even at optimal doping $x=0.15$.

To help understand this non-Drude response of σ_{xy} we examine the spin density wave (SDW) model previously used to analyze the σ_{xx} response and the dc Hall effect of PCCO.^{23,24} We consider a mean-field theory of electrons moving on a square lattice with dispersion

$$\begin{aligned} \varepsilon_p = & -2t(\cos p_x + \cos p_y) + 4t' \cos p_x \cos p_y \\ & - 2t''(\cos 2p_x + \cos 2p_y), \end{aligned} \quad (3)$$

and parameters $t=0.38 \text{ eV}=3056 \text{ cm}^{-1}$, $t'=0.32t$, and $t''=0.5t'$, chosen to reproduce the Fermi surface measured in the photoemission experiments.^{7,24} We assume that in addition to the dispersion [Eq. (3)] the electrons are coherently backscattered by a commensurate (π, π) spin density wave with gap amplitude Δ . The electric and magnetic fields are represented by vector potentials and coupled via the Peierls phase approximation, $\vec{p} \rightarrow \vec{p} - (e/c)\vec{A}$. At the relevant carrier concentrations, the Fermi surface is such that the scattering vector (π, π) connects Fermi surface points that become gapped and lead to reconstruction of the Fermi surface. If Δ is not too large ($\Delta < 0.26 \text{ eV}$ for $x=0.15$), the calculated Fermi surface exhibits both an electronlike pocket centered at $(\pi, 0)$ and holelike pockets centered at $(\pm\pi/2, \pi/2)$ as observed in ARPES;⁷ for larger Δ , only the electron pocket remains. The longitudinal and Hall conductivities are calculated by direct evaluation of the Kubo formula; for σ_{xy} we used the expressions given by Voruganti *et al.*²⁵ While this approach does not capture the physics of the Mott transition, it does give a reasonable picture of the effect of a SDW gap on the quasiparticle properties.

Using this model, the σ_{xy} response for $x=0.15$ and 0.12 is calculated using a constant scattering rate $\gamma=0.2t=608 \text{ cm}^{-1}$ and $\Delta=1200$ and 1800 cm^{-1} , respectively. The qualitative resemblance of the calculated curves to the data shown in Fig. 3 for $x=0.12$ and 0.15 is striking. In $\text{Im}(\sigma_{xy})$ a sign change occurs at a Δ -dependent frequency. Correspondingly, in the frequency range of interest (1000–3000 cm^{-1}), $\text{Re}(\sigma_{xy})$ becomes larger as Δ increases and two sign changes occur: one at high and one at low frequency. The zero crossing seen in $\text{Im}(\sigma_{xy})$ may be understood as follows. The SDW model predicts a Fermi surface made up of holelike and electronlike pockets. $\text{Im}(\sigma_{xy})$ is negative (electronlike) at low frequencies where the large electronlike pocket dominates the transport. However, at high frequency (frequencies much

higher than the SDW gap Δ), the response must revert to the holelike response of the underlying holelike band structure. Although the qualitative correspondence between calculation and data is excellent, an important difference exists: the magnitude of the calculated Hall response is larger than the measured values by factors of the order of 5. We believe this difference is the signature of the suppression of the ac charge response by Mott physics which we further address at the end of this discussion. Understanding this more precisely is an important open problem.

We now discuss limitations of the extended Drude model and SDW model that we used to interpret our results. To do so we will first discuss the temperature evolution of $\text{Im}(\sigma_{xy})$ for $x=0.12$ and 0.15 in Fig. 4 in terms of the SDW model. We will then examine results on the overdoped sample $x=0.18$ sample, which shows no SDW features, in terms of the conductivity sum rules.

While ARPES (Ref. 8) and IR σ_{xx} (Ref. 5) measurements indicate a complete closing of the SDW gap by $T=300$ K for $x=0.15$ and $x=0.12$, we see that for the $x=0.15$ sample the zero crossing of $\text{Im}(\sigma_{xy})$ only shifts slightly to lower frequencies [see lower arrow in Fig. 4(b)] below the measured frequency range as the temperature is raised. For $x=0.12$, the low-frequency response becomes less negative as temperature is raised [see the arrow in Fig. 4(c)]. Both these variations indicate only a partial closing of the high-energy pseudogap, contrary to its complete closing as seen by other spectroscopic techniques.^{5,9} This high-temperature incompatibility with the closing of a SDW gap has also been noticed in dc Hall measurements.¹¹

At high doping $x=0.18$, where no high-frequency SDW gap is observed, it becomes possible to analyze the effects of Mott physics on the Drude-like response. To do so we have estimated the optical sum rules of σ_{xy} . Indeed, sum rules have previously been very useful in revealing Mott physics in the σ_{xx} response of strongly interacting electron materials.²⁶ For σ_{xx} , the appropriate partial sum is

$$K(\Omega) = \int_0^\Omega \frac{2}{\pi} \text{Re}[\sigma_{xx}(\omega)] d\omega \quad (4)$$

and is proportional to the quasiparticle kinetic energy. In high- T_c superconductors, theoretical and experimental evidence suggests that for a cutoff frequency $\Omega=0.4$ eV, i.e., well above the Drude peak (seen from 0 to 0.1 eV) but well below the interband and upper Hubbard band features (seen above 1 eV), one finds the following relation:²⁶

$$K(0.4 \text{ eV}) \approx xK_{\text{band}}, \quad (5)$$

where $K_{\text{band}} \approx 0.4$ eV is the band theory conduction band kinetic energy and x is the doping (electron or hole) density per Cu atom. For frequencies below Ω , the response is Fermi-liquid-like and the extended Drude parametrization

$$\sigma_{xx}(\omega) = \frac{K_{\text{Mott}}}{\gamma_{xx}(\omega) - i\omega[1 + \lambda_{xx}(\omega)]} \quad (6)$$

is physically meaningful, where $K_{\text{Mott}} \approx K(0.4 \text{ eV})$.

For the Hall conductivity, the appropriate partial sum is²⁷

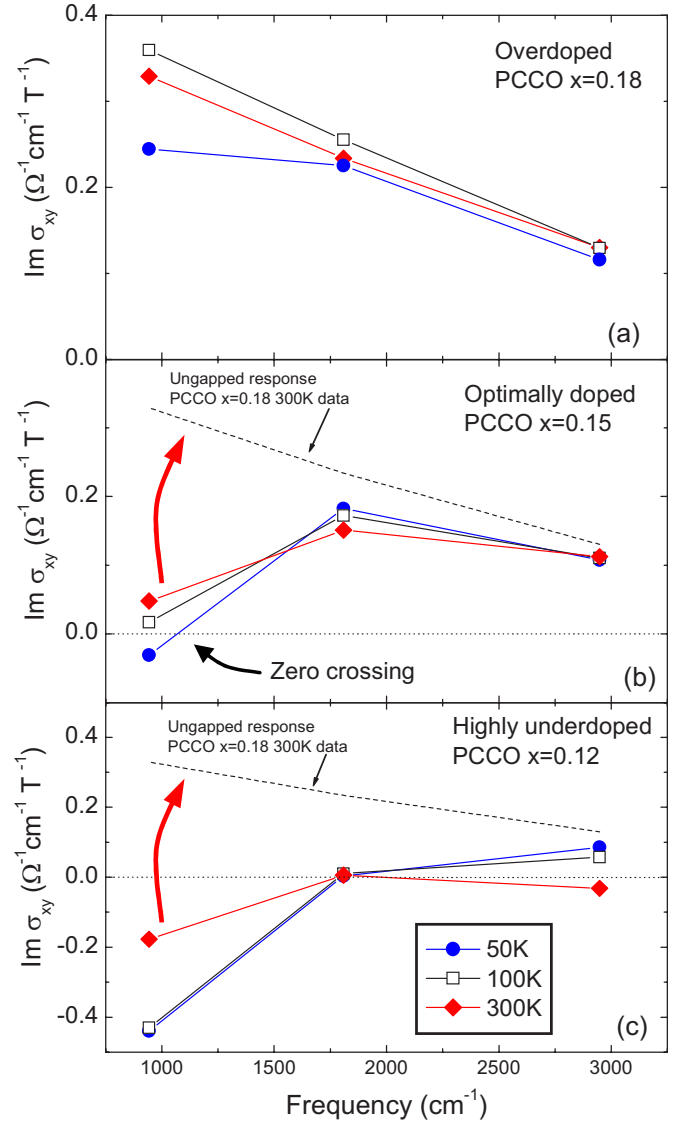


FIG. 4. (Color online) Temperature evolution of $\text{Im}(\sigma_{xy})$ for $x=0.18$, 0.15 , and 0.12 samples. As the temperature is raised, the optimally doped and underdoped samples shift only slightly toward what one would expect if the SDW gap completely closed [see red (gray) arrows], i.e., the simple extended Drude behavior represented in (b) and (c) by superimposing the $x=0.18$ 300 K data (dashed lines). Thus, contrary to ARPES and σ_{xx} results, the SDW does not appear to close in σ_{xy} measurements as the temperature is raised.

$$S(\Omega) = \int_0^\Omega \frac{2}{\pi} \omega \text{Im}[\sigma_{xy}(\omega)] d\omega \quad (7)$$

and the corresponding extended Drude parametrization is

$$\sigma_{xy}(\omega) = \frac{S_{\text{Mott}}}{\{\gamma_{xy}(\omega) - i\omega[1 + \lambda_{xy}(\omega)]\}^2}. \quad (8)$$

We can estimate $S([0.1;0.4] \text{ eV}) = \int_{0.1 \text{ eV}}^{0.4 \text{ eV}}$ directly from the data, finding about $0.045S_{\text{band}}$. We may estimate the contribution coming from below our measurement range $S(0 \text{ eV}, 0.1 \text{ eV})$ in two independent ways, which yield consistent answers.

First, we observe that the very low-frequency longitudinal conductivity is characterized by a “Drude peak” of width $\gamma_{xx} \approx 0.01$ eV at 25 K and a Hall resistance not too far from the band value, suggesting that, at low frequencies, a picture of weakly scattered quasiparticles is appropriate, so that $\gamma_{xy} = \gamma_{xx}$, allowing us to estimate the integral over the low-frequency region as

$$S(0.1 \text{ eV}) = \int_0^{0.1 \text{ eV}} \frac{2}{\pi} \omega \text{Im}[\sigma_{xy}(\omega)] d\omega \approx \frac{S_{\text{Mott}}}{[1 + \lambda_{xy}(\omega=0)]^2} \\ \approx \frac{\sigma_{xy}(\omega=0)}{(\gamma_{xx})^2} \approx 0.035 S_{\text{band}}, \quad (9)$$

leading to the estimate

$$S(0.4 \text{ eV}) = S(0.1 \text{ eV}) + S([0.1; 0.4] \text{ eV}) \approx 0.08 S_{\text{band}}. \quad (10)$$

The presence of any low-frequency electronlike contributions to $\text{Im}(\sigma_{xy})$ arising from antiferromagnetic fluctuations effects, as discussed earlier, would only decrease this estimation.

Second, model calculations²⁸ show that in the frequency range $\Omega \sim 0.2$ eV the quantity $\{\Omega/(\text{Im}[\sigma_{xy}(\Omega)]^{-1/2})^2\}$ is about a factor of 2 larger than $S(\Omega)$. Using this factor of 2 and our data, we find the estimate $S(0.4 \text{ eV}) \approx 0.1 S_{\text{band}}$.

To summarize, from the longitudinal conductivity one finds²³

$$K(0.4 \text{ eV}) \approx 0.18 K_{\text{band}}, \quad (11)$$

and from the transverse conductivity

$$S(0.4 \text{ eV}) \approx 0.1 S_{\text{band}}. \quad (12)$$

Thus, we conclude that the ir Hall data at $x=0.18$ imply a suppression of the σ_{xy} approximately a factor of 2 greater than the suppression of the longitudinal conductivity. This suggests different Mott renormalizations of the Hall and longitudinal conductivities. Refining these experimental estimates and extending them to other materials, as well as developing an appropriate body of theoretical results, may provide important insights into strongly correlated electron systems near the Mott transition.

We have reported the transverse optical conductivity $\sigma_{xy}(\omega)$ of the electron-doped cuprate $\text{Pr}_{2-x}\text{Ce}_x\text{CuO}_4$. At low temperatures, the results provide strong additional evidence for a spin density wave gap up to optimal doping and none at higher dopings. For underdoped and optimally doped samples ($x=0.12, 0.15$) the ir Hall data implies that the SDW gap is not fully closed even at $T=300$ K. In addition, at high dopings, a spectral weight analysis indicates that Mott correlation effects on the low-frequency Hall conductivity are still present and are even stronger than for the longitudinal conductivity.

The authors thank S. Dhar for Rutherford backscattering and channeling measurements and Y. Dagan for his initial work on film preparation using LSGO substrates. We acknowledge useful discussions with A. V. Chubukov and H. Kontani. The work at the University of Maryland was supported by NSF Grant Nos. DMR-0352735 and DMR-0303112. The work at the University at Buffalo was supported by the Research Corporation and NSF Grant No. CAREER-DMR0449899. A.J.M. and J.L. acknowledge support from NSF Grant No. DMR-0403167.

*Deceased.

†hdrew@physics.umd.edu

¹M. Imada, A. Fujimori, and Y. Tokura, *Rev. Mod. Phys.* **70**, 1039 (1998).

²P. K. Mang, O. P. Vajk, A. Arvanitaki, J. W. Lynn, and M. Greven, *Phys. Rev. Lett.* **93**, 027002 (2004).

³E. M. Motoyama, G. Yu, I. M. Vishik, O. P. Vajk, P. K. Mang, and M. Greven, *Nature (London)* **445**, 186 (2007).

⁴T. Uefuji, T. Kubo, K. Yamada, M. Fujita, K. Kurahashi, I. Watanabe, and K. Nagamine, *Physica C* **357-360**, 208 (2001).

⁵A. Zimmers, J. M. Tomczak, R. P. S. M. Lobo, N. Bontemps, C. P. Hill, M. C. Barr, Y. Dagan, R. L. Greene, A. J. Millis, and C. C. Homes, *Europhys. Lett.* **70**, 225 (2005).

⁶Y. Onose, Y. Taguchi, K. Ishizaka, and Y. Tokura, *Phys. Rev. B* **69**, 024504 (2004).

⁷N. P. Armitage, F. Ronning, D. H. Lu, C. Kim, A. Damascelli, K. M. Shen, D. L. Feng, H. Eisaki, Z.-S. Shen, P. K. Mang, N. Kaneko, M. Greven, Y. Onose, Y. Taguchi, and Y. Tokura, *Phys. Rev. Lett.* **88**, 257001 (2002).

⁸H. Matsui, K. Terashima, T. Sato, T. Takahashi, S. C. Wang, H. B. Yang, H. Ding, T. Uefuji, and K. Yamada, *Phys. Rev. Lett.* **94**, 047005 (2005).

⁹H. Matsui, T. Takahashi, T. Sato, K. Terashima, H. Ding, T. Uefuji, and K. Yamada, *Phys. Rev. B* **75**, 224514 (2007).

¹⁰A low-energy pseudogap has also been observed in these materials (Ref. 12). Contrary to the high-energy pseudogap we are interested in, this one opens just above T_c and is comparable in energy to the superconducting energy gap.

¹¹Y. Dagan, M. M. Qazilbash, C. P. Hill, V. N. Kulkarni, and R. L. Greene, *Phys. Rev. Lett.* **92**, 167001 (2004).

¹²L. Alff, Y. Krockenberger, B. Welter, M. Schonecke, R. Gross, D. Manske, and M. Naito, *Nature (London)* **422**, 698 (2003).

¹³L. B. Rigal, D. C. Schmadel, H. D. Drew, B. Maiorov, E. Osquigil, J. S. Preston, R. Hughes, and G. D. Gu, *Phys. Rev. Lett.* **93**, 137002 (2004).

¹⁴M. Grayson, L. B. Rigal, D. C. Schmadel, H. D. Drew, and P. J. Kung, *Phys. Rev. Lett.* **89**, 037003 (2002).

¹⁵J. Cerne, M. Grayson, D. C. Schmadel, G. S. Jenkins, H. D. Drew, R. Hughes, A. Dabkowski, J. S. Preston, and P.-J. Kung, *Phys. Rev. Lett.* **84**, 3418 (2000).

¹⁶E. Maiser, P. Fournier, J. L. Peng, F. M. Araujo-Moreira, T. Venkatesan, R. L. Greene, and G. Czjzek, *Physica C* **297**, 15 (1998).

¹⁷ R and T were measured at zero field. Recent high-magnetic-field experiments revealed that the magnetic field dependence of σ_{xx} up to 30 T is negligible (Ref. 19).

¹⁸Using previously published $\sigma_{xx}(\omega)$ data (Ref. 5), it is possible to reasonably extend our σ_{xx} curves down to 950 cm^{-1} . This extension is necessary when converting the complex Faraday angle to

- $\sigma_{xy}(\omega)$. We estimate that the uncertainty in the σ_{xx} extension generates less than a 1% error in the σ_{xy} data in Figs. 2 and 4.
- ¹⁹N. Margankunte, A. Zimmers, D. B. Tanner, R. L. Greene, and Y. J. Wang, in *24th International Conference on Low Temperature Physics-LT24*, AIP Conference Proceedings No. 850 (AIP Melville, NY, 2006), pp. 527-528.
- ²⁰J. Cerne, D. C. Schmadel, L. Rigal, and H. D. Drew, *Rev. Sci. Instrum.* **74**, 4755 (2003).
- ²¹M.-H. Kim, G. Acbas, M.-H. Yang, I. Ohkubo, H. Christen, D. Mandrus, M. A. Scarpulla, O. D. Dubon, Z. Schlesinger, P. Khalifah, and J. Cerne, *Phys. Rev. B* **75**, 214416 (2007).
- ²²J. Cerne, D. C. Schmadel, M. Grayson, G. S. Jenkins, J. R. Simpson, and H. D. Drew, *Phys. Rev. B* **61**, 8133 (2000).
- ²³A. Zimmers, J. M. Tomczak, R. P. S. M. Lobo, N. Bontemps, C. P. Hill, M. C. Barr, Y. Dagan, R. L. Greene, A. J. Millis, and C. C. Homes, *Europhys. Lett.* **70**, 224 (2005).
- ²⁴J. Lin and A. J. Millis, *Phys. Rev. B* **72**, 214506 (2005).
- ²⁵P. Voruganti, A. Golubentsev, and S. John, *Phys. Rev. B* **45**, 13945 (1992).
- ²⁶A. J. Millis, A. Zimmers, R. P. S. M. Lobo, N. Bontemps, and C. C. Homes, *Phys. Rev. B* **72**, 224517 (2005).
- ²⁷H. D. Drew and P. Coleman, R. P. S. M. Lobo, N. Bontemps, and C. C. Homes, *Phys. Rev. Lett.* **78**, 1572 (1997).
- ²⁸J. Lin and A. J. Millis (unpublished).